BRAIN
ORIGINAL ARTICLE

Disease-modifying effects of *TMEM106B* in genetic frontotemporal dementia: a longitudinal GENFI study

Saira S. Mirza,[1,2,†] Maurice Pasternak,[1,†] Andrew D. Paterson,[3] Ekaterina Rogaeva,[4] Maria C. Tartaglia,[4,5,6] Sara B. Mitchell,[6] Sandra E. Black,[1,2,6,7] Morris Freedman,[6,7] David Tang-Wai,[6,7,8] Arabella Bouzigues,[9] Lucy L. Russell,[9] Phoebe H. Foster,[9] Eve Ferry-Bolder,[9] Martina Bocchetta,[9] David M. Cash,[9] Henrik Zetterberg,[9,10,11,12] Aitana Sogorb-Esteve,[9,13] John van Swieten,[14] Lize C. Jiskoot,[14] Harro Seelaar,[14] Raquel Sanchez-Valle,[15] Robert Laforce Jr,[16] Caroline Graff,[17,18] Daniela Galimberti,[19,20] Rik Vandenberghe,[21,22] Alexandre de Mendonça,[23] Pietro Tiraboschi,[24] Isabel Santana,[25,26] Alexander Gerhard,[27,28] Johannes Levin,[29,30,31] Sandro Sorbi,[32,33] Markus Otto,[34] Florence Pasquier,[35,36] Simon Ducharme,[37,38] Chris Butler,[39,40] Isabelle Le Ber,[41,42] Elizabeth Finger,[43] James B. Rowe,[44] Matthis Synofzik,[45,46] Fermin Moreno,[47,48,49] Barbara Borroni,[50] Jonathan D. Rohrer[9] and Mario Masellis[1,2,6] on behalf of the GENetic Frontotemporal dementia Initiative (GENFI)

[†]These authors contributed equally to this work.

Common variants within *TMEM106B* are associated with risk for frontotemporal lobar degeneration with TDP-43 pathology (FTLD-TDP). The G allele of the top single nucleotide polymorphism, *rs1990622*, confers protection against FTLD-TDP, including genetic cases due to *GRN* mutations or *C9orf72* hexanucleotide repeat expansions. However, the effects of interaction between *TMEM106B-rs1990622* and frontotemporal dementia (FTD) mutations on disease endophenotypes in genetic FTD are unknown.

This longitudinal cohort study was embedded within the GENetic Frontotemporal dementia Initiative (GENFI). We included 518 participants from 222 families [209 non-carriers; 222 presymptomatic carriers (*C9orf72* = 79; *GRN* = 101, *MAPT* = 42); 87 symptomatic carriers (*C9orf72* = 45; *GRN* = 29; *MAPT* = 13)] followed for up to 7 years. Using linear mixed-effects models, we examined the effects of a triple interaction between *TMEM106B-rs1990622*^{G} allele dosage (additive model: 0, 1 or 2 alleles) and autosomal dominant FTD mutations with clinical status, and time from baseline on (i) grey matter volume using a voxel-based analysis; (ii) serum neurofilament light chain (NfL) levels; and (iii) cognitive and behavioural measures.

Mean age of participants was 47.9 ± 13.8 years, 58.1% were female and 61% had at least one G allele. *C9orf72*: *rs1990622*^{G} allele dosage was associated with less atrophy within the right occipital region in presymptomatic carriers at baseline, and reduced atrophy rate within putamen and caudate nucleus, right frontotemporal regions, left cingulate and bilateral insular cortices in symptomatic carriers over time; lower NfL levels in presymptomatic carriers at baseline; better executive functions and language abilities in presymptomatic carriers; and maintained overall cognitive functions and behaviour in symptomatic carriers over time. *GRN: rs1990622*^{G} allele dosage was associated with

Received July 04, 2024. Revised October 31, 2024. Accepted December 14, 2024. Advance access publication April 22, 2025

reduced grey matter atrophy rate within the right temporal and occipital regions in presymptomatic carriers, and within the right frontal cortex and insula over time in symptomatic carriers; lower serum NfL levels over time in presymptomatic carriers and lower NfL levels at both baseline and over time in symptomatic carriers; and better global cognitive performance at baseline and higher attention/processing speed scores over time in symptomatic carriers. *MAPT*: *rs1990622*^{G} allele dosage was associated with reduced grey matter atrophy rate within the right inferior frontal gyrus in symptomatic carriers, but no effects on serum NfL or cognitive/behavioural measures.
TMEM106B-rs1990622^{G} allele dosage showed protective effects on multiple endophenotypes predominantly in *GRN* and *C9orf72* groups. Therefore, *TMEM106B* genotype should be assessed in clinical trials, particularly of *GRN*- and *C9orf72*-related genetic FTD, due to its modifying effects on biomarker, imaging, cognitive and clinical outcomes.

1 Centre for Brain Resilience and Recovery, Hurvitz Brain Sciences Research Program, Sunnybrook Research Institute, University of Toronto, Toronto, ON M4N 3M5, Canada
2 L. C. Campbell Cognitive Neurology Research Unit, Sunnybrook Health Sciences Centre, Toronto, ON M4N 3M5, Canada
3 Program in Genetics and Genome Biology, The Hospital for Sick Children, Toronto, ON M5G 1E8, Canada
4 Tanz Centre for Research in Neurodegenerative Diseases, University of Toronto, Toronto, ON M5S 1A8, Canada
5 Memory Clinic, University Health Network, Toronto, ON M5T 2S8, Canada
6 Division of Neurology, Department of Medicine, University of Toronto, Toronto, ON M5S 3H2, Canada
7 Rotman Research Institute, Baycrest Health Sciences, Toronto, ON M6A 2E1, Canada
8 Krembil Research Institute, University Health Network, Toronto, ON M5T 2S8, Canada
9 Dementia Research Centre, Department of Neurodegenerative Disease, UCL Queen Square Institute of Neurology, University College London, London WC1N 3AR, UK
10 Department of Psychiatry and Neurochemistry, University of Gothenburg, Gothenburg 405 30, Sweden
11 Clinical Chemistry, Sahlgrenska University Hospital, Gothenburg 413 45, Sweden
12 DRI Fluid Biomarker Laboratory, Hong Kong Center for Neurodegenerative Diseases, Clear Water Bay, Hong Kong 999 077, China
13 UK Dementia Research Institute at University College London, London NW1 3BT, UK
14 Department of Neurology, Erasmus Medical Center, Rotterdam 3015 GD, The Netherlands
15 Alzheimer's disease and Other Cognitive Disorders Unit, Neurology Service, Hospital Clínic, Institut d'Investigacións Biomèdiques August Pi I Sunyer, University of Barcelona, Barcelona 08036, Spain
16 Clinique Interdisciplinaire de Mémoire, Département des Sciences Neurologiques, CHU de Québec, and Faculté de Médecine, Université Laval, Quebec, QC G1V 4G2, Canada
17 Department of Neurobiology, Care Sciences and Society; Center for Alzheimer Research, Division of Neurogeriatrics, Bioclinicum, Karolinska Institutet, Solna 171 65, Sweden
18 Unit for Hereditary Dementias, Theme Inflammation and Aging, Karolinska University Hospital, Stockholm SE-171 76, Sweden
19 Fondazione Ca' Granda, IRCCS Ospedale Policlinico, Milan 20122, Italy
20 Department of Biomedical, Surgical and Dental Sciences, University of Milan, Centro Dino Ferrari, Milan 20122, Italy
21 Laboratory for Cognitive Neurology, Department of Neurosciences, KU Leuven, Leuven 3001, Belgium
22 Neurology Service, University Hospitals Leuven, Leuven 3000, Belgium
23 Faculty of Medicine, University of Lisbon, Lisbon 1649-028, Portugal
24 Dipartimento Diagnostica e Tecnologia - Neurologia V, Fondazione IRCCS Istituto Neurologico Carlo Besta, Milano 20133, Italy
25 Faculty of Medicine, University of Coimbra, Coimbra 3004-531, Portugal
26 Centre for Innovative Biomedicine and Biotechnology (CIBB), University of Coimbra, Coimbra 3004-531, Portugal
27 Division of Psychology Communication and Human Neuroscience, Wolfson Molecular Imaging Centre, University of Manchester, Manchester M20 3LJ, UK
28 Department of Nuclear Medicine, Center for Translational Neuro- and Behavioural Sciences, University Medicine Essen, Essen 45147, Germany
29 Department of Neurology, Ludwig-Maximilians Universität München, Munich 80802, Germany
30 Clinical Study Unit, German Center for Neurodegenerative Diseases (DZNE), Munich 81377, Germany
31 Munich Cluster for Systems Neurology (SyNergy), Munich 81377, Germany
32 Department of Neurofarba, University of Florence, Florence 50139, Italy
33 Department of Neurology, IRCCS Fondazione Don Carlo Gnocchi, Florence 50139, Italy
34 Department of Neurology, University of Ulm, ULM 45 89081, Germany
35 Division of Neurology, Faculty of Medicine, Univ Lille, Lille 59000, France
36 Lille Neurosciences and Cognition, Inserm 1172, Lille 59000, France
37 Douglas Mental Health University Institute, Department of Psychiatry, McGill University, Montreal, QC H4H 1R3, Canada

38 McConnell Brain Imaging Centre, Montreal Neurological Institute, McGill University, Montreal, QC H4H 1R3, Canada
39 Nuffield Department of Clinical Neurosciences, Medical Sciences Division, University of Oxford, Oxford OX3 7JX, UK
40 Department of Brain Sciences, Imperial College London, London SW7 2AZ, UK
41 Sorbonne Université, Paris Brain Institute—Institut du Cerveau—ICM, Inserm U1127, CNRS UMR 7225, AP-HP—Hôpital Pitié-Salpêtrière, Paris 75013, France
42 Centre de référence des démences rares ou précoces, IM2A, Département de Neurologie, AP-HP—Hôpital Pitié-Salpêtrière, Paris 75013, France
43 Department of Clinical Neurological Sciences, University of Western Ontario, London, ON N6A 3K7, Canada
44 Department of Clinical Neurosciences and Cambridge University Hospitals NHS Trust, University of Cambridge, Cambridge, CB2 3EB, UK
45 Department of Neurodegenerative Diseases, Hertie-Institute for Clinical Brain Research and Center of Neurology, University of Tübingen, Tübingen 72076, Germany
46 Faculty of Medicine, Center for Neurodegenerative Diseases (DZNE), Tübingen 72076, Germany
47 Cognitive Disorders Unit, Department of Neurology, Hospital Universitario Donostia, Donostia, Gipuzkoa 20014, Spain
48 Center for Biomedical Research in Neurodegenerative Disease (CIBERNED), Carlos III Health Institute, Madrid 28029, Spain
49 Biogipuzkoa Health Research Institute, Neurosciences Area, Group of Neurodegenerative Diseases, San Sebastian 20014, Spain
50 Neurology Unit, Department of Clinical and Experimental Sciences, University of Brescia, Brescia 15–25121, Italy

Correspondence to: Mario Masellis, MSc, MD, PhD, FRCPC
Professor of Medicine (Neurology), University of Toronto; Cognitive & Movement Disorders Clinic
Cognitive Neurology Research Unit, Sunnybrook Health Sciences Centre
2075 Bayview Ave., Room A4-42, Toronto, Ontario M4N 3M5, Canada
E-mail: mario.masellis@sunnybrook.ca

Keywords: additive model; *TMEM106B*; FTLD-TDP; blood-based biomarkers; cognition; structural MRI

Introduction

Frontotemporal dementia (FTD) represents a group of clinically and pathologically heterogeneous neurodegenerative disorders with neuronal loss primarily in the frontal and temporal lobes. This leads to profound changes in behaviour and language abilities.[1] Approximately one-third of FTD cases show autosomal dominant inheritance and the majority is attributable to mutations in three genes: chromosome 9 open reading frame 72 (*C9orf72*),[2,3] progranulin (*GRN*),[4,5] and microtubule-associated protein tau (*MAPT*).[6] On autopsy of genetic FTD, the two most common pathologies include: Tau-positive inclusions (FTLD-Tau), associated with mutations in *MAPT*, and TDP-43 positive inclusions (FTLD-TDP) associated with *GRN* and *C9orf72* mutations.[7]

Genetic FTD shows clinical heterogeneity,[8] variable age at onset, particularly for *GRN* and *C9orf72* mutations, and variable disease duration.[9,10] Imaging biomarkers show partially overlapping patterns of grey and white matter loss, and regional cerebral hypoperfusion,[11] across *C9orf72*, *MAPT* and *GRN* mutation carriers compared with non-carriers.[12,13] This partial overlap translates into neuropsychological endophenotypes, with the dominant cognitive profiles differing between FTD genetic groups both at presentation and longitudinally.[14] FTD genetic cases also share elevated blood levels of neurofilament light chain (NfL), albeit with wide variability between groups.[15] Serum NfL has emerged as a proximity biomarker of neuroaxonal degeneration as increasing levels in presymptomatic individuals harbouring FTD mutations may predict short-term risk of conversion to clinical FTD.[16] The temporal order of imaging, NfL and cognition changes in genetic FTD differs by genetic group.[17]

While there are currently no approved disease-modifying therapies for genetic FTD, several drug candidates are being evaluated in clinical trials.[1,18] Knowledge of the natural progression of FTD and the identification of factors that modify its course are crucial for the effective implementation of these therapeutics, ideally during the prodromal stages when irrecoverable neuronal damage has not occurred. Furthermore, therapeutic strategies may arise from exploiting protective genetic mechanisms.[19,20]

Van Deerlin and colleagues' genome-wide association study[21] (GWAS) identified genetic risk factors for FTLD-TDP from 2509 control subjects and 515 cases with pathologically confirmed FTLD-TDP, some of which had *GRN* mutations. Three single nucleotide polymorphisms (SNPs) in high linkage disequilibrium spanning *TMEM106B* on chromosome 7p21.3 were associated with FTLD-TDP.[21] For the top SNP (*rs1990622*), the alternate G allele was protective [$P = 1.08 \times 10^{-11}$; odds ratio (OR) = 0.61, 95% confidence interval (CI): 0.53–0.71]. This was replicated in a second pathologically confirmed FTLD-TDP case-control cohort, although not in a smaller cohort of FTD cases with unspecified pathology.[22] Stratification of this GWAS sample on presence of *GRN* mutations showed protective effects of *TMEM106B* in both *GRN*-positive and *GRN*-negative groups, but the effect was stronger in *GRN* mutation carriers. However, a formal interaction between *TMEM106B-rs1990622* and *GRN* was not tested.[21] An independent replication study showed

nominal associations of the three *TMEM106B* SNPs with FTD risk in a cohort of 640 cases and 822 controls.[23] The majority of cases included in this GWAS were living, thus of unknown pathological subtype. However, when the sample was stratified on *GRN* mutations, protective effects of *TMEM106B* were stronger.[23] This study suggested a recessive model, i.e. two G alleles confer protection against *GRN*-associated FTLD-TDP. There is also a modifying role of *TMEM106B* in *C9orf72* expansion carriers.[24] Subsequent studies have replicated these findings in other *GRN* cohorts,[25-27] in those with *C9orf72* repeat expansions,[24,28] and in undifferentiated clinical FTD.[22,29] Clinically diagnosed FTD patients of British origin failed to replicate the GWAS findings from 470 cases.[30] However, this study excluded patients with known *GRN* or *MAPT* mutations.

The reference allele (A) for *rs1990622* is detrimental. In a clinically diagnosed FTD cohort of 198 patients, including 31 genetic cases, lower cortical volumes were shown in the frontal ($P = 0.009$), temporal ($P = 0.029$), cingulate ($P = 0.014$) and insular ($P = 0.018$) lobes in $rs1990622^{AA}$ compared to $rs1990622^{AG/GG}$.[31] The population-based Rotterdam Study ($n = 4413$) examined associations between $rs1990622^{A}$ and regional cortical volumes and reported reduced grey matter volume of left-sided temporal brain regions, including the superior temporal gyrus ($\beta = -88.8$ µl per risk allele, $P = 7.64 \times 10^{-5}$).[32] In terms of cognitive outcomes, $rs1990622^{A}$ was shown to be associated with greater decline in Mini-Mental State Examination (MMSE) score in persons with FTD [minor-allele dominant model ($\beta = 0.969$, $P = 0.001$)],[33] and in those with Parkinson's disease [co-dominant model ($\beta = 0.123$, $P = 0.019$)].[33] Furthermore, *TMEM106B-rs1990622*^{A} influences age of onset in *GRN* carriers.[34] While these studies support the role of the *TMEM106B-rs1990622* as an important genetic factor for disease modification, they are mostly cross-sectional with limited sample sizes, have largely focused on one genetic group, and do not examine the presymptomatic stages of genetic FTD. In contrast, while the GWAS datasets are large, they have extremely limited clinical and endophenotype information and do not reveal potential mechanisms underlying the disease modification effects. Findings from relevant literature are summarized in Supplementary Table 1.

In summary, protective effects of *TMEM106B-rs1990622*^{G} have been mostly observed in FTLD-TDP, especially in the *GRN* group. However, effects are also shown in *C9orf72* and other patient groups,[33] and in healthy individuals.[32] Furthermore, insoluble amyloid fibrils of TMEM106B protein were identified in post-mortem human brains afflicted with TDP-43 proteinopathies, tauopathies, or α-synucleinopathies, thus indicating a putative role for its pathological fibrillization across different neurodegenerative diseases.[35] In this large longitudinal multimodal study of a cohort of individuals with/or at risk for genetic FTD, we therefore examined the interactive effects between *TMEM106B-rs1990622* and *GRN*, *C9orf72* or *MAPT* mutations, along with clinical status, on brain imaging, serum biomarker, as well as cognitive and behavioural measures commonly used in FTD clinical trials. We hypothesized that protective effects of *TMEM106B-rs1990622*^{G} would be mainly seen in groups with FTLD-TDP pathology, specifically, *GRN* and *C9orf72*, and that effects would be more pronounced in *GRN* mutation carriers.

Materials and methods

In families segregating *C9orf72* repeat expansions or *GRN* or *MAPT* mutations, we examined if *TMEM106B-rs1990622* modifies the effect of these mutations on: (i) grey matter volume; (ii) serum NfL; and (iii) cognitive and behavioural measures, at baseline and longitudinally, accounting for FTD clinical status, i.e. presymptomatic versus symptomatic FTD.

Setting and study population

Data were drawn from the multicentre GENetic Frontotemporal dementia Initiative (GENFI) study, which recruits members of families segregating pathogenic mutations in *C9orf72*, *GRN* or *MAPT*, thus allowing tracking of the evolution of genetic FTD from its earliest stages.[36] The pilot phase of GENFI, 'GENFI 1' (2012 to 2015), recruited 365 participants from 13 sites across Europe and Canada. The second phase, 'GENFI 2' (2015 to 2021), recruited 1000 participants from 25 sites. The current study includes data from GENFI 1 and GENFI 2. The asymptomatic family members of symptomatic index cases (i.e. symptomatic carriers) could either be non-carriers (i.e. controls) or carriers (i.e. presymptomatic) of an autosomal dominant mutation in any of the three main FTD genes. All participants were genotyped for these genes at their local site, with a pathogenic expansion in *C9orf72* defined as ≥30 repeats.[3]

At each annual visit, participants underwent a standardized clinical assessment, including a neuropsychological battery[36] and brain MRI.[13] Blood was collected at baseline and longitudinally for biomarker assessment, including NfL, and for genomic analysis. Ethical review boards from all sites approved the study protocol and all participating individuals provided written and informed consent in agreement with the Declaration of Helsinki.

DNA samples were available for 589 persons from the GENFI datafreeze 6 (GENFI 1 and 2) recruited and followed between January 2012 and January 2021. We included 518 participants with phenotype data from 222 families (209 non-carrier controls, 222 presymptomatic carriers, 87 symptomatic carriers) (Table 1). Brain MRI, serum NfL and neuropsychological data were available at baseline and up to seven annual follow-up visits.

The number of participants at baseline and follow-up by *TMEM106B* genotype and FTD genetic groups for imaging, NfL and cognition data are shown in Supplementary Table 2.

Genotyping

Blood or DNA samples from GENFI participants were collected from all sites by the central UCL coordinating site and sent to the Tanz Centre for Neurodegenerative Diseases (University of Toronto) for DNA extraction and biobanking (E.R.). Five hundred and eighty-nine samples were genotyped on NeuroChip (Infinium Core-24 +v1.2 Kit, Illumina, Inc.) at the Clinical Genomics Centre (Toronto, Canada). The NeuroChip includes known common and rare variants associated with all major neurodegenerative diseases as well as a GWAS backbone.[37] Three samples with call rate < 98% were removed. SNPs with a call frequency < 0.85 and a GenTrain score < 0.7, with cluster separation < 0.2 were also excluded.

Data were sent to Sunnybrook Research Institute for quality control (QC) and analyses (S.S.M., M.M., A.D.P.). SNPs with a call rate of <95% and a minor allele frequency of <0.05 were removed; sex discrepant cases ($n = 10$) and heterozygosity outliers ($n = 8$) were excluded using *PLINK* 1.9.[38] Relatedness and family structure was examined in detail using Kinship Inference in Genomics (*KING* 2.3.1).[39] Population stratification was examined using multi-dimensional scaling in *KING* [GENFI samples were projected to the 1000 Genomes' principal component (PC) space], and confirmed with *GrafPop*.[40] Ancestry inference results from both *KING* and

Table 1 Baseline characteristics of study sample by *TMEM106B-rs1990622*

	Characteristic	*TMEM106B-rs1990622*^{AA} $n = 203$	*TMEM106B-rs1990622*^{AG} $n = 251$	*TMEM106B-rs1990622*^{GG} $n = 64$	P-value
Non-carrier controls, $n = 209$	*n*	87 (41.6%)	102 (48.8%)	20 (9.6%)	
	Sex (female)	54 (62%)	56 (55%)	14 (70%)	0.36
	Age	47.18 ± 14.35	45.07 ± 12.39	47.05 ± 10.49	0.52
	Education, years	13.86 ± 3.22	14.49 ± 3.32	13.0 ± 3.85	0.14
	TIV, l	1.46 ± 0.14	1.50 ± 0.15	1.49 ± 0.14	0.08
C9orf72 presymptomatic, $n = 79$	*n*	30 (38%)	37 (46.8%)	12 (15.2%)	
	Sex (female)	17 (57%)	25 (68%)	8 (67%)	0.63
	Age	45.59 ± 12.67	43.21 ± 10.72	51.14 ± 14.04	0.14
	Education, years	15.00 ± 2.70	13.73 ± 2.41	14.25 ± 3.14	0.15
	TIV, l	1.48 ± 0.14	1.48 ± 0.16	1.41 ± 0.87	0.09
C9orf72 symptomatic, $n = 45$	*n*	18 (40%)	17 (37.8%)	10 (22.2%)	
	Sex (female)	10 (56%)	3 (18%)	4 (40%)	0.07
	Age	64.58 ± 7.22	65.0 ± 6.57	65.36 ± 9.06	0.96
	Education, years	13.61 ± 3.38	13.53 ± 2.90	11.1 ± 5.82	0.22
	TIV, l	1.48 ± 0.14	1.58 ± 0.15	1.56 ± 0.18	0.14
	Age of onset	59.50 ± 7.75	59.47 ± 7.41	59.70 ± 10.23	0.99
GRN presymptomatic, $n = 101$	*n*	38 (37.6%)	57 (56.4%)	6 (5.9%)	
	Sex (female)	26 (68%)	33 (58%)	3 (50%)	0.20
	Age	45.38 ± 13.39	43.56 ± 10.26	46.06 ± 14.15	0.71
	Education, years	15.56 ± 3.59	14.40 ± 3.50	13.66 ± 3.20	0.21
	TIV, l	1.48 ± 0.18	1.49 ± 0.15	1.55 ± 0.16	0.54
GRN symptomatic, $n = 29$	*n*	15 (51.7%)	11 (37.9%)	3 (10.3%)	
	Sex (female)	8 (53%)	5 (45%)	2 (67%)	0.81
	Age	65.80 ± 8.87	61.12 ± 7.87	66.70 ± 6.29	0.33
	Education, years	11.30 ± 3.90	11.63 ± 3.85	11.0 ± 3.0	0.91
	TIV, l	1.41 ± 143	1.47 ± 195	1.49 ±0.17	0.55
	Age of onset	63.53 ± 8.74	57.82 ± 7.85	64.33 ± 7.23	0.20
MAPT presymptomatic, $n = 42$	*n*	10 (23.8%)	22 (52.4%)	10 (23.8%)	
	Sex (female)	7 (70%)	17 (77%)	4 (40%)	0.11
	Age	37.95 ± 10.84	35.65 ± 9.07	45.91 ± 10.74	0.06
	Education, years	12.5 ± 3.87	14.9 ± 3.4	14.2 ± 2.0	0.17
	TIV, l	1.45 ± 0.13	1.41 ± 0.19	1.51 ± 0.19	0.38
MAPT symptomatic, $n = 13$	*n*	5 (38.5%)	5 (38.5%)	3 (23.1%)	
	Sex (female)	1 (20%)	3 (60%)	2 (67%)	0.47
	Age	61.60 ± 6.44	55.17 ± 3.05	65.03 ± 3.28	**0.02**
	Education, years	9.80 ± 3.42	12.80 ± 3.83	18.33 ± 1.53	**0.01**
	TIV, l	1.45 ± 0.13	1.43 ± 0.14	1.37 ± 0.14	0.79
	Age of onset	55.2 ± 5.63	49.5 ± 0.71	48.5 ± 4.95	0.32

Values are means (standard deviation) or counts (percentage). *P*-values are derived from ANOVA for continuous and chi-squared or Fisher's exact test for categorical variables. Significant *P*-values are indicated in bold. TIV = total intracranial volume, in litres.

GrafPop showed that the majority of participants had a European origin, and identified three ethnic outliers, which were excluded. PCs were calculated using the *PC-AiR*[41] option from the GENetic estimation and inference in structured samples (GENESIS)[42] programme, using genotype data on unrelated individuals and unrelated SNPs (LD-pruned). Scree plots[43] were used to determine the number of significant PCs; first three PCs were retained to be used as covariates in the analyses to account for potential population stratification effects. Detailed genomic QC procedures are presented in the Supplementary material, 'Methods' section. After QC, genotype data ($n = 565$) were imputed against the TOPMed reference panel version 2, a diverse reference panel including information from 97 256 deeply sequenced human genomes.[44]

TMEM106B allele dosage definition

TMEM106B-rs1990622 genotype data (chromosome 7; position: 12244161; frequencies: reference/risk allele A = 0.63, alternate/protective allele G = 0.37) were extracted from imputed data (imputed SNP; $R^2 = 0.99$) and coded into allele dosage with reference to the G allele (0 = AA; 1 = AG; 2 = GG). We used an additive model, i.e. *TMEM106B-rs1990622*^{G} dosage of 0, 1 and 2 was used as a continuous variable to test associations of *rs1990622* with endophenotypes of interest. Deviations from the additive model were examined by testing a heterozygous indicator (AG = 1; AA and GG = 0) in the model along with the *TMEM106B-rs1990622*^{G} dosage variable. No deviations from an additive effect were observed for any phenotype (heterozygosity indicator $P > 0.05$). Hardy-Weinberg Equilibrium was tested separately in all study groups after removing related individuals (one individual per family included). Hardy-Weinberg equilibrium was maintained across all groups (Supplementary Table 3).

Structural MRI data

Volumetric T_1-weighted MRI was performed on 3 T or 1.5 T scanners at sites where 3 T scanning was not available in GENFI 1. Participants were scanned at their local site on one of the three

different platforms (Philips Healthcare, GE Healthcare Life Sciences, Siemens Healthcare Diagnostics). Standard scan protocols were designed at the outset of the study to match across scanners as much as possible.[36] Volumetric T_1-weighted images were processed for 380 participants who had scans at a minimum of two time points using *CAT12*'s longitudinal segmentation pipeline using Geodesic Shooting for spatial registration and normalization to the MNI152 non-linear 2009c template.[45,46] One hundred and thirty-eight participants had scans at one time point only, and were processed using *CAT12*'s cross-sectional segmentation pipeline.[45] Partial grey matter volume output from both pipelines were merged and used to generate a population mask by averaging voxel-wise and thresholding to a grey matter partial volume ≥0.2. These volumes were also smoothed prior to voxel-based morphometry (VBM) using a 10 mm full-width at half-maximum (FWHM) Gaussian kernel to reduce nuisance effects from imperfect alignment. Total intracranial volume (TIV; presented in Table 1) was calculated within each *CAT12* pipeline automatically.[47] Based on *CAT12*'s image quality rating score (out of 100%), seven data-points were below the rating of 70% due to artefacts such as motion, and were excluded from the VBM analysis (final participant $n = 517$ for VBM analysis). This included loss of three scans belonging to one subject, removing all imaging data for this participant. Four scans were also removed, one each from four subjects, who all had multiple scans.

Serum neurofilament light chain data

Blood was collected by venipuncture in serum-separating tubes and centrifuged (2000*g* for 10 min) at room temperature within 3 h of withdrawal, according to a standardized GENFI protocol. After centrifugation, serum was stored in aliquots at −80°C until use according to standardized procedures. Participants were not instructed to fast and time of day at blood collection was variable. On the serum from participants included in this study, NfL (pg/ml) was measured in duplicate in longitudinal samples collected. Samples were measured using the Single molecule array (Simoa) NF-Light Advantage Kit (Quanterix;) on an HD-1 Analyzer following the manufacturer's instructions. The lower limit of detection of the assay for NfL was 0.104 pg/ml. Measurements were carried out at the same study site on consecutive days. To keep sample processing and plating consistent, serum samples were thawed at room temperature for 2 h and subsequently centrifuged at 10 000*g* for 5 min; 150 µl samples were aliquoted in a 96-well plate (Quanterix) and frozen at −80°C until analysis. Quality control samples had a mean intra-assay and inter-assay coefficient of variation of <10%, and samples with a coefficient of variation of >15% were re-measured. Samples were analysed in nine runs, with longitudinal samples of each participant measured in the same run. Laboratory technicians were blinded to all clinical and genetic information.[48]

Neuropsychological and behavioural data

Trained neuropsychologists blinded to neuroimaging, administered the neuropsychological tests.[36] Composite scores for the following domains were calculated by averaging the z-scores of relevant neuropsychological test scores:[14] attention and processing speed [Wechsler Memory Scale–Revised (WMS-R) Digit span (DS) forward,[49] Trail Making Test (TMT) part-A[50] and Wechsler Adult Intelligence Scale–Revised (WAIS-R) Digit Symbol test][49]; executive function (WMS-R DS backward, TMT part-B, and phonemic fluency)[51]; Language [Boston Naming Test (BNT, short 30 item version)[49] and category fluency (animals)].[51] Block design test[52] was used for visuospatial function and MMSE[53] for global cognition. For memory assessment, different tests were employed in GENFI 1 (Logical Memory Test)[54] and GENFI 2 (Free and Cued Selective Reminding Test),[55] which could not be combined as they target different subprocesses and are also influenced differentially by other cognitive processes, such as executive function.[56] The revised version of the Cambridge Behaviour Inventory (CBI-R) was used to assess behavioural impairment. CBI-R is a 45-item questionnaire completed by an informant assessing the frequency of the given behaviour over the past month on a scale of 0–4.[57] Higher scores represent more severe behavioural deficits (max score = 180). Total CBI-R raw scores were used in analyses.

Variables

Main predictor variables included gene-clinical status (non-carrier controls, presymptomatic *C9orf72* carriers, symptomatic *C9orf72* carriers, presymptomatic *GRN* carriers, symptomatic *GRN* carriers, presymptomatic *MAPT* carriers, or symptomatic *MAPT* carriers), and *TMEM106B* allele dosage. Covariates included age at baseline, sex, scanner site and TIV (imaging outcomes only) and years of education (cognitive outcomes only). Analyses included time from baseline in years and random intercepts clustered over subjects nested within family to account for repeated measures data and familial relatedness of the subjects.

See Supplementary Table 4 for detailed family information including numbers and sizes of *C9orf72*, *GRN* and *MAPT* families.

Statistical analyses

Composite scores for cognition

Neuropsychological test scores were standardized to create z-scores (z-score: raw score – mean score controls at baseline/SD controls at baseline).[14] Test scores assessing performance time, i.e. TMT-A and -B were inversed so that lower scores indicate worse cognitive function, as for all other tests.

Participant characteristics at baseline were compared across *TMEM106B-rs1990622* genotypes in all gene-clinical groups using ANOVA for continuous and chi-squared or Fisher's exact tests for categorical variables.

Model specification

To test the interaction effects of *TMEM106B-rs1990622* with autosomal dominant FTD mutations on grey matter volume, serum NfL levels, cognition and behaviour, we used the following R-style formula for linear mixed effects models (LMMs):

$$\begin{aligned} Brain\ volume \sim\ & rs1990622 \times Group \times Time_{from\ baseline} \\ & + Age_{at\ baseline} + Sex + Site + TIV \\ & + (1 \mid Family\ /\ Subject) \end{aligned} \quad (1)$$

$$\begin{aligned} NfL \sim\ & rs1990622 \times Group \times Time_{from\ baseline} + Age_{at\ baseline} + Sex \\ & + (1 \mid Family\ /\ Subject) \end{aligned} \quad (2)$$

$$\begin{aligned} Cognition\ or\ Behaviour \sim\ & rs1990622 \times Group \times Time_{from\ baseline} \\ & + Age_{at\ baseline} + Sex + Education_{years} \\ & + (1 \mid Family\ /\ Subject) \end{aligned} \quad (3)$$

The term '*rs1990622* × Group × Time from Baseline' denotes main and interaction effects of these variables. *rs1990622*^{G} allele dosage (0 = AA, 1 = AG, 2 = GG) is used as a continuous term, i.e. an additive model. 'Group' denotes the gene-clinical variable (e.g. non-carrier control as the reference level, *GRN* + presymptomatic, *GRN* + symptomatic, *C9orf72* + presymptomatic, *C9orf72* + symptomatic, *MAPT* + presymptomatic, or *MAPT* + symptomatic); and '(1 | Family/Subject)' denotes random intercepts assigned to both subjects and families where subjects are nested within families. The LMMs were run to test the hypotheses that *TMEM106B-rs1990622* modulates the effect of FTD mutation in each of the gene-clinical groups (six contrasts for each slope and baseline comparison) each compared to the control group, both at baseline (Time 0) and longitudinally.

Linear mixed effects VBM analysis was performed using *AFNI's version 24.0.88*[58] *3dLMEr* module.[59] For serum NfL and cognition analyses, model fitting and hypothesis testing were performed using *R* version 4.2.3 using the *lmer* (1.1–35.3), and *emmeans* (1.10.2) packages, respectively. All analyses were corrected for multiple testing (see later for VBM analyses). Cognition and behaviour analyses were corrected for six tests using Bonferroni correction.

Differences in grey matter volumes, serum NfL and cognitive and CBI-R scores between *rs1990622*^{G} allele dosage both at baseline and over time (slope differences) were derived from the LMMs.

NfL, cognition and behavioural results are presented as β-coefficients per G allele with 95% CI. β-Coefficients and corresponding *P*-values for baseline are β-coefficients and *P*-values for a double interaction between *rs1990622*^{G} allele dosage and gene-clinical group at baseline time = 0. β-Coefficients and corresponding *P*-values for longitudinal analyses (slopes) are β-coefficients and *P*-values for a triple interaction between *rs1990622*^{G} allele dosage, gene-clinical group and time from baseline.

Voxel-based morphometry analyses

For structural MRI analysis, linear mixed effects VBM analysis was performed using AFNI's version 24.0.88[58] *3dLMEr* module.[59] This leverages a local R installation and its packages ensuring that LMMs were fit with the same R (4.2.3), *lmer* (1.1–35.3), and *emmeans* (1.10.2) versions. Model residuals were utilized to calculate the spatial autocorrelation of the output statistical maps using *AFNI's 3dFWHMx* program.[60] These spatial autocorrelation parameters along with a voxel-wise threshold of $P < 8.33 \times 10^{-5}$ ($P < 8.33 \times 10^{-5}$ is derived by: 0.001/12 for the 12 contrasts tested, i.e. six cross-sectional contrasts and six longitudinal contrasts) were used as input to AFNI's 3dClustSim program to arrive at a $P < 0.001$ family-wise error (FWE)-corrected cluster threshold. Additionally, we selected the strictest definition that voxels must have had complete cubic-face contact (i.e. edge-only and/or vertex-only voxel connections were not considered valid). A resulting threshold of 370 contiguous voxels represented clusters that survived $P < 0.001$ FWE. Corrected clusters were resampled and mapped against a 3D render of an MNI152 template brain using *MRICroGL*.[61] Cluster summaries were generated by inputting the corrected cluster images through the atlasreader Python package.[62] VBM results are reported as partial grey matter volume units (pGM), which are representations of the proportions of tissues that occupy a given brain voxel. For example, if a particular voxel has partial volume units of 0.2, 0.8 and 0 for grey matter, white matter and CSF, respectively, then it is interpreted as 20% of the voxel being occupied by grey matter and 80% being occupied by white matter.

VBM results are presented as difference in partial grey matter volume (ΔpGM) for baseline and ΔpGM/year for longitudinal analyses. Baseline estimates are results of an interaction between *TMEM106B-rs1990622*^{G} allele dosage and gene-clinical status at baseline time = 0, whereas longitudinal estimates (slopes) are result of a triple interaction between *TMEM106B-rs1990622*^{G} allele dosage, gene-clinical status and time from baseline.

Secondary/*post hoc* analyses

To examine the protective effects of *rs1990622*^{G} on memory, we performed a secondary analysis in the GENFI 2 subsample (n = 281, 54% of full sample) using the FCSRT total delayed recall score (Supplementary material, 'Methods' section).

In a secondary survival analysis, we examined the association of *rs1990622*^{G} with risk of conversion to clinical FTD in presymptomatic *C9orf72*, *GRN* and *MAPT* carriers, using *GRN-TMEM106B*^{AA} as reference. Cox proportional hazards models adjusted for age, sex and education were used to calculate hazard ratios (HRs), when possible (Supplementary material, 'Methods' section).

We also performed a *post hoc* analysis to further examine the protective effects of *rs1990622*^{G}. We divided the presymptomatic group into two subgroups: mutation carriers who converted (converters), and mutation carriers who did not convert and are past their expected age of symptom onset (past EASO). Briefly, the EASO for a given participant was defined as the difference between the age at baseline evaluation minus mean age of disease onset within the family for that participant.[11] We compared endophenotypes using LMMs between these groups per gene (Supplementary material, 'Methods' section).

Finally, to test any potential effects of population stratification, or MRI scanner change during follow-up, we derived the mean values of regions of interest (ROIs) from significant clusters of the main VBM analysis, and ran: (i) ROI, NfL and MMSE models additionally adjusting for the first three PCs in a stepwise fashion to account for potential population stratification; and (ii) ROI models additionally adjusting for a variable indicating MRI scanner change (yes versus no) to account for the effect of scanner change during follow-up. We formally tested model improvement by the Akaike and Bayesian Information Criteria (AIC and BIC) and the log-likelihood ratio test taken together. ROIs were extracted because VBM models could not be compared as AFNI's *3dLMEr* module does not allow model comparisons.

Results

The analyses included 518 participants followed for up to 7 years. The *MAPT* symptomatic group showed significant differences in age and education across the *rs1990622* genotypes (Table 1).

Grey matter volumes: VBM analyses

C9orf72

At baseline, the presymptomatic *C9orf72* carriers were the only group to demonstrate protective effects of *rs1990622*^{G} allele dosage, where less atrophy was seen in the right calcarine cortex in an additive manner (Table 2). However, longitudinally, no protective effect of *rs1990622*^{G} allele on grey matter atrophy rate was observed in this group (Table 3). Within the symptomatic *C9orf72* group, *TMEM106B-rs1990622*^{G} allele dosage was associated with lower atrophy over time in several cortical and subcortical regions in an additive manner. The largest cluster (8896 mm^3) comprised the putamen, caudate nucleus, and insular cortex in the left hemisphere. Other clusters showing less atrophy over time within the

Table 2 Clusters showing greater grey matter volume associated with *TMEM106B-rs1990622*^{G} allele dosage at baseline

Group	Cluster number	Cluster size (mm^3)	Cluster mean Z-value	Cluster peak Z-value	Mean effect value per G allele (ΔpGM)[a]	MNI Peak Coordinates			Anatomical structures[b]
						x	y	z	
C9orf72 presymptomatic	1	1306.12	4.19	4.60	0.04	9	−73.5	10.5	Right calcarine cortex
C9orf72 symptomatic	No significant clusters								
GRN presymptomatic	No significant clusters								
GRN symptomatic	No significant clusters								

Clusters of voxels derived from VBM linear mixed-effects models where less atrophy was observed associated with *TMEM106B-rs1990622*^{G} allele cross-sectionally.
[a]ΔpGM = difference in partial grey matter volume. Estimates derived from a voxel-wise map of an interaction between *TMEM106B-rs1990622*^{G} allele dosage and gene-clinical status at time from baseline = 0.
[b]Anatomical structures as per Harvard-Oxford Atlas.

symptomatic *C9orf72* group included right putamen and frontotemporal cortices, left cingulate cortex, and bilateral insular cortices (Fig. 1 and Table 3). *rs1990622*^{G} allele dosage was associated with a reduction in atrophy rate of 0.006 to 0.012 ΔpGM per G allele/year, reported over cluster averages (Table 3).

GRN

At baseline, we did not observe any protective effects of *rs1990622*^{G} allele dosage on atrophy in either the presymptomatic or the symptomatic *GRN* group. Longitudinally, in presymptomatic *GRN* carriers, *rs1990622*^{G} allele dosage was associated with reduced rates of atrophy in widespread areas around the right hemispheric temporo-occipital structures in an additive manner (Fig. 1 and Table 3). The magnitude of the protective effect ranged from 0.004 to 0.006 ΔpGM per G allele/year (Table 3). Protective effects of *rs1990622*^{G} allele were even stronger in the symptomatic *GRN* carriers, and ranged from 0.013 to 0.02 ΔpGM per G allele/year. The largest identified mega-cluster with a cluster size of 90 926 mm^3 showed significantly reduced atrophy rate in the right insula, left anterior cingulate cortex and superior frontal gyrus, and the putamen bilaterally, associated with *rs1990622*^{G} allele dosage. The other three clusters showing protective effects of *rs1990622*^{G} allele dosage longitudinally included several frontal lobe structures in the right hemisphere (Fig. 1 and Table 3).

MAPT

The *MAPT* group showed no protective effects of *TMEM106B-rs1990622*^{G} at baseline. Longitudinally, only the symptomatic *MAPT* carriers showed reduced atrophy rate in the right inferior frontal gyrus (Fig. 1 and Table 3).

Serum neurofilament light chain

At baseline, presymptomatic *C9orf72* carriers showed lower NfL levels associated with *rs1990622*^{G} allele dosage; however, no effects were seen longitudinally in any *C9orf72* group (Fig. 2). Within the *GRN* mutation carriers, the presymptomatic group showed significantly lower NfL levels associated with *rs1990622*^{G} allele dosage (β for slope per G allele: −3.10; 95% CI: −4.75, −1.39; *P*: 0.0003) over time, but not at baseline (Fig. 2). However, in the symptomatic *GRN* group, not only *rs1990622*^{G} allele dosage was associated with significantly lower serum NfL levels (β per G allele: −27.86; 95% CI: −37.44, −18.30; *P*: 2.53×10^{-8}) at baseline, but over time as well (β for slope per G allele: −6.43; 95% CI: −10.43, −2.43; *P*: 0.002). No effects of *rs1990622*^{G} on serum NfL were observed in the *MAPT* group (Fig. 2).

Cognition and behaviour

At baseline, after Bonferroni correction, protective effects of *rs1990622*^{G} allele dosage were observed in the symptomatic *GRN* carriers only, and that was for global cognition (β per G allele: 2.16, 95% CI: 2.27, 5.61, corrected *P*: 2.59×10^{-5}) (Fig. 3 and Table 4).

Longitudinally, within the presymptomatic *C9orf72* carriers, *rs1990622*^{G} allele dosage was associated with significantly better executive functions (β for slope per G allele: 0.09, 95% CI: 0.03, 0.15, corrected *P*: 0.01) and language scores (β for slope per G allele: 0.11, 95% CI: 0.04, 0.19, corrected *P*: 0.024) over time (Fig. 3 and Table 4). Within the symptomatic *C9orf72* group, *rs1990622*^{G} allele dosage was associated with a stronger protective effect longitudinally on behaviour as measured by CBI-R, global cognition, and all cognitive domains except for visuospatial (Fig. 3 and Table 4).

In symptomatic *GRN* carriers longitudinally, *rs1990622*^{G} allele dosage was associated with a significantly higher attention and processing speed score (β for slope per G allele: 0.28; 95% CI: 0.09, 0.46; corrected *P*: 0.02) over time. No longitudinal protective effect was observed in the *GRN* presymptomatic group. No *GRN* groups showed any protective effects of *rs1990622*^{G} on behaviour as measured by the CBI-R.

MAPT groups did not show any effects of *rs1990622*^{G} on cognition nor behaviour.

For detailed LMMs outputs including double and triple interaction *P*-values and coefficients of each variable (NfL, cognition and behavioural analyses), refer to Supplementary Tables 5 and 6.

Secondary/*post hoc* analyses

We did not find any significant protective effects of *TMEM106B* on memory in any of the gene groups at baseline or over time (Supplementary Table 7).

Survival analysis included 222 individuals with 21 conversion events over 717 person-years. The *GRN-TMEM106B*^{GG} group did not have any converters over a mean follow-up of 4 years; the *GRN-TMEM106B*^{AG} group had a significantly lower risk of conversion (HR: 0.22; 95% CI: 0.05, 0.98; *P*-value: 0.046) compared to *GRN-TMEM106B*^{AA} (Supplementary Table 8 and Fig. 1).

Post hoc analyses showed that for serum NfL, the past EASO *GRN* group had lower levels of serum NfL over time than their converter counterparts in association with *rs1990622*^{G}. For the left insular volume, both *C9orf72* and *GRN* past EASO groups showed less atrophy over time compared to their converter counterparts in association with *rs1990622*^{G} (Supplementary Table 9).

Model improvements were not observed after additionally adjusting for the first PC (i.e. population stratification effects) in the ROI, NfL or MMSE models (Supplementary Table 10), or adjusting the ROI

Table 3 Clusters showing less atrophy rate associated with *TMEM106B-rs1990622*^{G} allele dosage over time

Group	Cluster number	Cluster size (mm^3)	Cluster mean Z-value	Cluster peak Z-value	Mean effect value (ΔpGM per G allele/year)[a]	MNI peak coordinates			Anatomical structures[b]
						x	y	z	
C9orf72 presymptomatic					No significant clusters				
C9orf72 symptomatic	1	8896.5	5.01	7.92	0.01	−10.5	15	−1.5	Left putamen; left caudate nucleus; left insula
	2	7303.5	4.54	6.23	0.006	64.5	−24	27	Right supramarginal gyrus; right superior temporal gyrus; right middle temporal gyrus
	3	2126.2	4.25	5.09	0.006	21	12	−3	Right putamen; right insula
	4	1663.87	4.79	6.76	0.012	52.5	36	1.5	Right inferior frontal triangular gyrus; right inferior frontal orbital gyrus
	5	1542.37	4.33	4.92	0.008	−10.5	−52.5	33	Left precuneus; left middle cingulate cortex; left posterior cingulate cortex
GRN presymptomatic	1	2254.5	4.45	5.29	0.004	63	−19.5	19.5	Right superior temporal gyrus; right rolandic operculum; right supramarginal gyrus; right postcentral gyrus
	2	1788.75	4.31	5.03	0.005	31.5	−79.5	37.5	Right superior occipital gyrus; right middle occipital gyrus
	3	1653.75	4.45	5.77	0.006	49.5	−46.5	16.5	Right superior temporal gyrus; right middle temporal gyrus
GRN symptomatic	1	90 925.87	5.29	12.70	0.02	−10.5	15	−3	Right insula; left putamen; left anterior cingulate cortex; left superior frontal gyrus, medial part; right putamen
	2	4333.5	4.45	5.82	0.02	24	61.5	−16.5	Right anterior orbitofrontal cortex; right medial frontal orbital gyrus; right superior frontal dorsolateral gyrus; right superior medial frontal gyrus
	3	4070.25	4.34	5.37	0.02	18	43.5	49.5	Right middle frontal gyrus; right superior frontal dorsolateral gyrus; right superior medial frontal gyrus
	4	1248.75	4.38	5.15	0.013	49.5	7.5	19.5	Right inferior frontal operculum; right precentral gyrus
MAPT presymptomatic					No significant clusters				
MAPT symptomatic	1	1711.12	4.93	7.10	0.01	57	27	−3	Right inferior frontal orbital gyrus; right inferior frontal triangular gyrus

Clusters of voxels derived from VBM linear mixed-effects models where less atrophy rate was observed associated with *TMEM106B-rs1990622*^{G} allele dosage longitudinally.

[a]ΔpGM/year = difference in partial grey matter volume per year. Estimates derived from a voxel-wise map of a triple interaction between *TMEM106B-rs1990622*^{G} allele dosage, gene-clinical status, and time from baseline.

[b]Anatomical structures (as per Harvard-Oxford Atlas) are listed according to the cluster size in descending order.

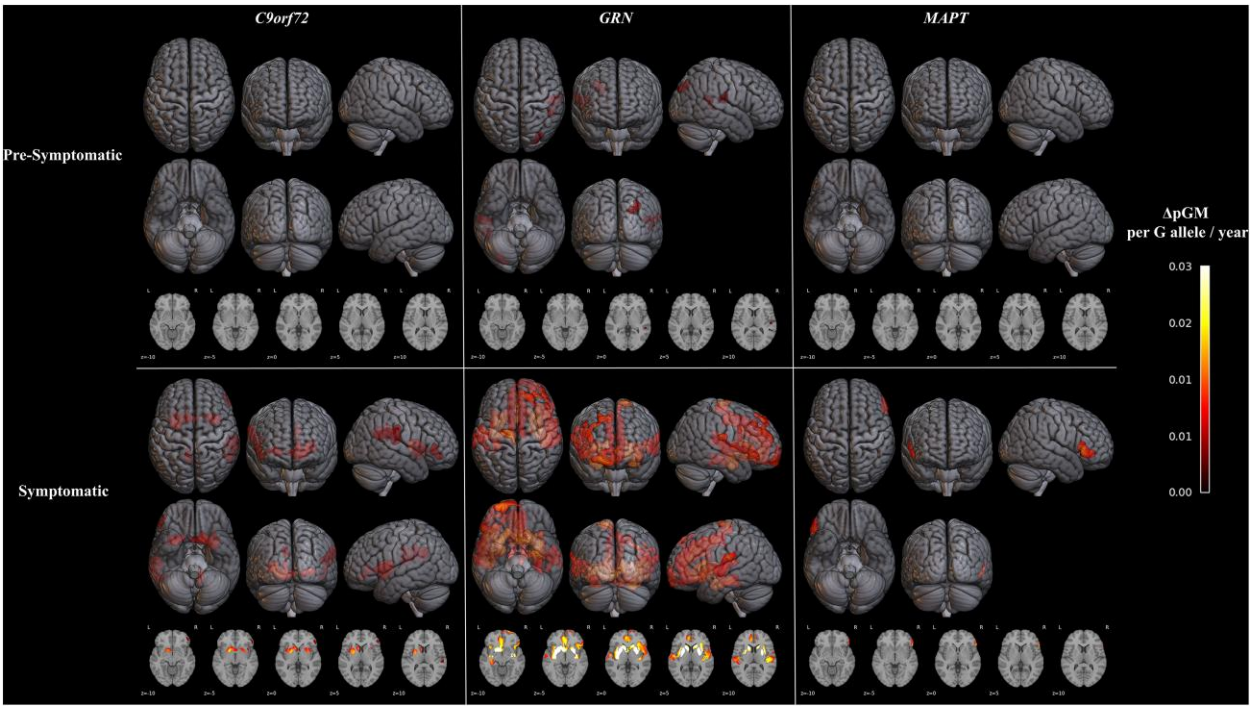

Figure 1 Longitudinal associations of *TMEM106B-rs1990622*^{G} allele dosage and brain volumes. The figure shows clusters of grey matter showing less atrophy rate associated with *TMEM106B-rs1990622*^{G} allele dosage over time. Results are derived from voxel-based morphology (VBM) linear mixed-effects models. Images are in neurological display convention. ΔpGM = difference in partial grey matter volume.

models for scanner change (Supplementary Table 11). Therefore, no further PCs were added.

Discussion

This multicentre longitudinal study demonstrated additive protective effects of the *TMEM106B-rs1990622*^{G} allele on grey matter volume, serum NfL levels, and cognition/behaviour in genetic FTD caused by mutations in *GRN* or *C9orf72* predicted to have FTLD-TDP neuropathology. For grey matter volume, *C9orf72* carriers showed some protective effects of *rs1990622*^{G} at baseline, but more so over time, whereas the *GRN* group showed more prominent protective effects of *rs1990622*^{G} over time only. For serum NfL, protective effects of *rs1990622*^{G} were observed mainly in *GRN* mutation carriers, both in presymptomatic and symptomatic groups. For cognition, the symptomatic *GRN* carriers showed strong protective effects of *rs1990622*^{G} on global cognition at baseline, and on attention and processing speed longitudinally, whereas the *C9orf72* group showed more generalized protective effects on cognition and behaviour longitudinally. The *MAPT* group (FTLD-Tau) showed no protective effects of *rs1990622*^{G} except for reduced atrophy rate in a small right inferior frontal region, supporting the hypothesis that *TMEM106B* modifies FTLD-TDP pathology more strongly.

Strengths include a good sample size for the primary analyses, use of multimodal data, longitudinal design, robust genomics and MRI processing pipeline and analytical methods, and inclusion of three FTD genetic groups associated with both FTLD-TDP and FTLD-Tau pathology. The genomics pipeline also included thorough examination and confirmation of relatedness and family structure. Population structure was examined and confirmed using multiple programmes to avoid any confounding due to population stratification. Importantly, we considered whether a mutation carrier was presymptomatic or symptomatic, accounting for known differences in the natural history of the different genetic disorders,[63] e.g. *C9orf72* repeat expansions have been associated with a longer psychiatric prodrome in many cases[64] and imaging changes are often seen earlier than in those with *GRN* mutations,[17] suggesting potential neurodevelopmental effects in *C9orf72*-related FTD.

The cross-sectional VBM results showed protective effects of *rs1990622*^{G} allele dosage within the right calcarine cortex (i.e. less atrophy) in presymptomatic *C9orf72* expansion carriers. However, no protective effect was observed in the symptomatic *C9orf72* group or any *GRN* carrier groups at baseline. Indeed, atrophy sets in much earlier in *C9orf72* expansion carriers prior to symptom onset compared to *GRN* mutation carriers,[36,63] which might explain why the presymptomatic *C9orf72* group showed an effect at baseline.

Longitudinal protective effects were stronger in *GRN* carriers than in *C9orf72* carriers; areas of reduced atrophy rate in the right frontal region were observed in all three gene groups, with the strongest effect in *GRN* followed by *C9orf72*, and a lesser effect in *MAPT*. Previously, the *rs1990622* risk allele has been shown to be associated with lower volume of the left superior temporal gyrus in healthy older adults,[32] and with greater decline in global cognition in Parkinson's disease,[33] suggesting that modifying effects of *TMEM106B* may also exist in non-FTLD-TDP cohorts, and healthy controls. It was indeed shown that TMEM106B amyloid protein fibrils were present in human brains confirmed to have not only TDP-43 proteinopathies, but also tauopathies and α-synucleinopathies.[35] This suggests a putative role for pathological fibrillization of TMEM106B across different neurodegenerative diseases,[35] and this is supported by our *MAPT* findings.

The observed protective *rs1990622*^{G} effects in our study involved anatomical structures routinely observed in genetic FTD disease

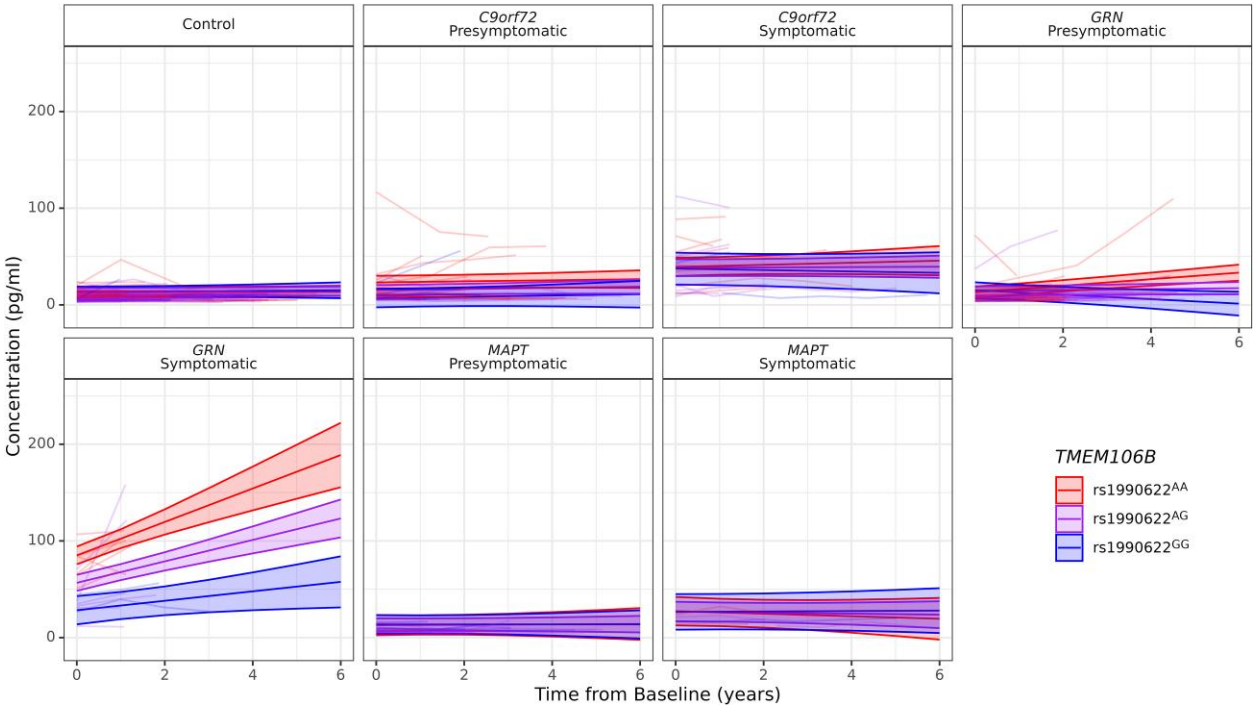

Figure 2 Associations of *TMEM106B-rs1990622*^{G} allele dosage and serum neurofilament light chain levels. Figure shows predicted serum neurofilament light chain (NfL) levels over time by *TMEM106B-rs1990622*^{G} allele dosage. Comparisons are derived from a single linear mixed effects model. Spaghetti plots in background show raw data. Significant differences: Baseline: (i) presymptomatic *C9orf72* [β^{int}: −7.57; 95% confidence interval (CI): −14.57, −0.57; P^{int}: 0.03]; (ii) symptomatic *GRN* (β^{int}: −27.86; 95% CI: −37.44, −18.30; P^{int}: 2.53×10^{-8}). Slope difference: (i) presymptomatic *GRN* (β^{int}: −3.10; 95% CI: −4.75, −1.39; P^{int}: 0.0003); (ii) symptomatic *GRN* (β^{int}: −6.43; 95% CI: −10.43, −2.43; P^{int}: 0.002). β^{int} and P^{int} at baseline: β and *P*-value for an interaction between *TMEM106B-rs1990622*^{G} allele dosage and gene-clinical status at time from baseline = 0. β^{int} and P^{int} over time: β and *P*-value for a triple interaction between *TMEM106B-rs1990622*^{G} allele dosage, gene-clinical status and time from baseline. See Supplementary Table 5 for complete outputs of the linear mixed-effects model including test statistics and degrees of freedom.

progression due to *C9orf72* and *GRN* mutations and areas of atrophy observed in a previous cross-sectional GENFI VBM study.[13] For instance, we observed protective effects of *TMEM106B-rs1990622*^{G} allele dosage in occipital regions in addition to fronto-temporal areas in *GRN* mutation carriers; parieto-occipital regions have been shown to be affected in symptomatic *GRN* carriers.[65] Insular, orbitofrontal and cingulate cortical volumes were relatively protected by *rs1990622*^{G} as evidenced by reduced atrophy rate in both symptomatic *C9orf72*, and presymptomatic and symptomatic *GRN* groups. These regions comprise major portions of the salience network, which degenerates as FTD progresses.[66,67]

Our VBM results largely translated into NfL findings (Fig. 2). In the presymptomatic *C9orf72* group at baseline, serum NfL levels were lower in *rs1990622*^{G} carriers; however, there was no difference in levels over time in this group. Perhaps a rise in serum NfL levels in *C9orf72* carriers commences near conversion or much later than in *GRN* carriers, which is why the protective effect was also not evident and not significant enough to be detected. *rs1990622*^{G} allele dosage was associated with significantly lower serum NfL levels in presymptomatic *GRN* carriers longitudinally, and this protective effect was even stronger in symptomatic carriers, providing evidence of less neurodegeneration. NfL rise in *C9orf72* mutation carriers is subtle and gradual, with the exception of amyotrophic lateral sclerosis (ALS), where higher levels are observed, likely because of the large-calibre axonal degeneration associated with ALS.[68] In contrast, *GRN* mutation carriers show low presymptomatic levels but major and sustained rise after clinical onset,[68] which might explain why we observed prominent protective effects only in *GRN* carriers.

At baseline, only the symptomatic *GRN* group showed protective effects of *rs1990622*^{G} allele dosage on global cognition, as measured by the MMSE. Remarkably, this strong protective effect on global cognition did not reflect into other domains in this group at baseline, but longitudinally protective effects were seen on attention and processing speed. The lack of protective effects on cognition in the presymptomatic *GRN* group can be explained by the slower pathological course in *GRN* mutation carriers during the presymptomatic stage, which are consistent with our VBM findings. While we did see strong protective effects of *rs1990622*^{G} in symptomatic *GRN* carriers regarding attention and processing speed longitudinally, this was not as extensive as in the *C9orf72* group across multiple cognitive domains. Several factors may explain this observation. First is the significant attrition related to disease severity in the symptomatic *GRN* group (Supplementary Table 2) compared to the symptomatic *C9orf72* group—*GRN* mutation carriers decline more slowly during the presymptomatic phase, but once symptomatic, they have a more rapid and severe decline than the *C9orf72* group, especially *rs1990622*^{AA} homozygotes. Therefore, there was less longitudinal data available in the *GRN* symptomatic group because they declined more quickly and could not be tested. Second, there were fewer *rs1990622*^{GG} homozygotes in the *GRN* symptomatic group as they were less likely to develop FTD in the first place. With a lower number of data-points available for follow-up, particularly for the *rs1990622*^{AA} subgroup because of dropouts, we believe that the symptomatic *GRN* group is statistically less powered to detect protective effects in our cognition analysis. Third, memory function was not tested in the full sample in our

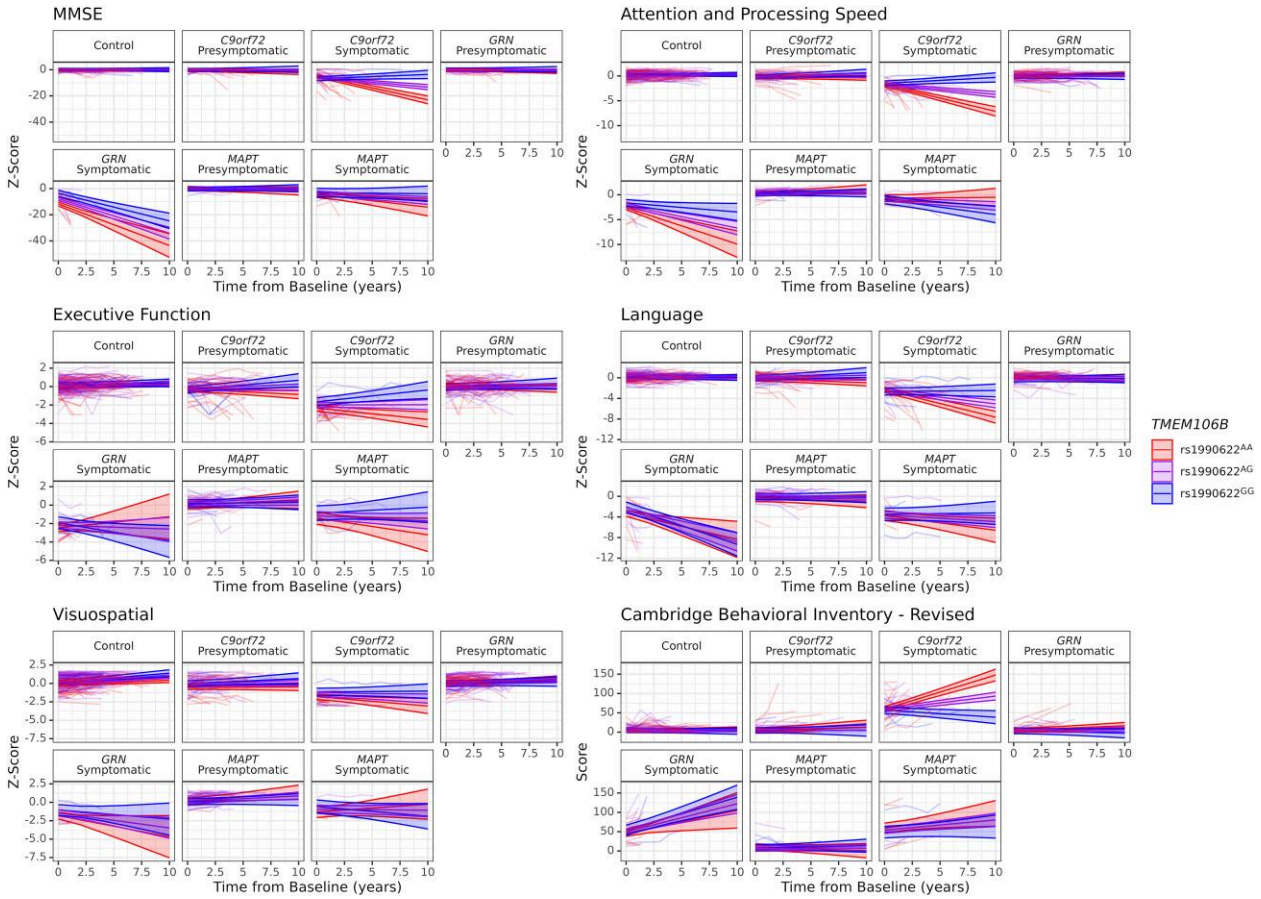

Figure 3 Associations of *TMEM106B-rs1990622*^{G} allele dosage with cognition and behaviour. Figure shows predicted cognitive composite, global cognition and Cambridge Behaviour Inventory-Revised (CBI-R) scores by *TMEM106B-rs1990622*^{G} allele dosage. Comparisons in each domain are derived from a single linear mixed-effects model per domain. Spaghetti plots in background show raw data. Refer to Supplementary Table 6 for complete outputs of the linear mixed-effects model, including test statistics and degrees of freedom.

study, and as patients with *GRN* mutations can also present with early episodic memory impairment,[69] this may not have been captured. Additionally, neuropsychological assessments are relatively less precise in comparison to structural imaging and biomarker measures, which are less prone to patient and extrinsic influences. These factors may explain why symptomatic *GRN* carriers show robust protective effects of *rs1990622*^{G} allele dosage on our VBM and serum NfL analyses, but less so on cognition.

With respect to behavioural changes, the symptomatic *C9orf72* group was the only group demonstrating additive protective effects of *rs1990622*^{G} on behaviour, as longitudinally measured by the CBI-R. It is known that *C9orf72* mutations are the most common genetic cause of familial and sporadic behavioural variant FTD (bvFTD).[70] Our data also showed that the majority (71%, 32/45) of *C9orf72* symptomatic patients had a bvFTD diagnosis compared to only 48% (14/29) having this diagnosis in the symptomatic *GRN* group. Furthermore, of all bvFTD cases in this GENFI sample, 54% (32/59) were *C9orf72* mutation carriers compared to only 24% (14/59) being *GRN* mutation carriers. In comparison, *GRN* symptomatic cases in GENFI more often presented with language impairment, wherein 80% (12/15) of all cases with primary progressive aphasia were *GRN* carriers (see Table 4 for diagnostic breakdown). Therefore, the higher prevalence of behavioural features in *C9orf72* symptomatic cases may explain our results.

TMEM106B belongs to the TMEM106 family of proteins with relatively unknown function. It is expressed in neurons, with some expression in glial and endothelial cells. Specifically, TMEM106B is a type 2 integral membrane glycoprotein predominantly located in the membranes of endosomes and lysosomes, and as lysosomes are integral to clearance of cell debris including proteins, their dysfunction has been closely linked to several neurodegenerative disorders. There is conflicting evidence on the role of *TMEM106B* expression in *GRN*-related disease. Higher *TMEM106B* mRNA expression[21] and protein levels[71] of TMEM106B have been shown in those with no protective *TMEM106B*^{G} allele in symptomatic *GRN* mutation carriers.[21] TMEM106B, when upregulated or overexpressed, results in improper lysosomal formation, poor lysosomal acidification, attenuated lysosomal transport, and increased lysosomal stress.[72] Conversely, in double knock-out models of *Tmem106b*$^{-/-}$ and *Grn*$^{-/-}$ mice, disease pathology was exacerbated along with accumulation of phosphorylated TDP-43 in an age-dependent manner.[73-75] Another study reported an increase in TDP-43 cytoplasmic aggregates in *Tmem106b* knock-out mice in a cellular model for TDP-43.[76] More work needs to be done to understand this complex relationship between *GRN* haploinsufficiency and *TMEM106B* expression.

Our multimodal data from GENFI provide evidence that *TMEM106B* genotype interacts with *C9orf72* and *GRN* mutations and—to a lesser extent—with *MAPT* mutations to modulate FTD endophenotypes. In contrast to our study, a cross-sectional GENFI study, which included 231 participants, reported that *TMEM106B* genotype did not alone affect grey matter volume on its own, but

Table 4 Associations of *TMEM106B-rs1990622*^{G} allele dosage and cognitive and behavioural scores at baseline and over time

	Difference at baseline		Difference in slope		Difference at baseline		Difference in slope	
	β^{int} per G allele (95% CI)	[a]Corrected *P*-value^{int}	β^{int} per G allele (95% CI)	[a]Corrected *P*-value^{int}	β^{int} per G allele (95% CI)	[a]Corrected *P*-value^{int}	β^{int} per G allele (95% CI)	[a]Corrected *P*-value^{int}
	***C9orf72* presymptomatic**				***C9orf72* symptomatic**			
Global cognition	−0.13 (−1.20, 0.93)	1.00	0.11 (−0.09, 0.31)	1.00	−1.16 (−2.38, 0.06)	0.36	1.06 (0.80, 1.32)	**2.19×10^{-14}**
Attention and processing speed	0.01 (−0.29, 0.31)	1.00	0.05 (−0.01, 0.11)	0.54	0.12 (−0.24, 0.47)	1.00	0.33 (0.25, 0.41)	**8.82×10^{-15}**
Executive functions	−0.19 (−0.48, 0.10)	1.00	0.09 (0.03, 0.15)	**0.01**	0.19 (−0.15, 0.52)	1.00	0.14 (0.06, 0.21)	**0.0018**
Language	−0.05 (−0.48, 0.38)	1.00	0.11 (0.04, 0.19)	**0.02**	−0.28 (−0.79, 0.23)	1.00	0.30 (0.20, 0.40)	**4.63×10^{-8}**
Visuospatial functions	0.10 (−0.22, 0.41)	1.00	−0.00001 (−0.06, 0.06)	1.00	0.15 (−0.22, 0.52)	1.00	0.04 (−0.05, 0.12)	1.00
CBI-R	−0.04 (−6.02, 5.95)	1.00	−0.62 (−1.82, 0.58)	1.00	−0.92 (−7.71, 5.87)	1.00	−5.13 (−6.49, −3.77)	**1.54×10^{-12}**
	***GRN* presymptomatic**				***GRN* symptomatic**			
Global cognition	−0.09 (−1.19, 1.01)	1.00	0.07 (−0.12, 0.25)	1.00	3.94 (2.27, 5.61)	2.59×10^{-5}	0.52 (−0.12, 1.16)	0.66
Attention and processing speed	−0.10 (−0.41, 0.20)	1.00	−0.01 (−0.07, 0.04)	1.00	0.45 (−0.004, 0.90)	0.30	0.28 (0.09, 0.46)	**0.02**
Executive functions	−0.16 (−0.46, 0.14)	1.00	0.04 (−0.02, 0.09)	1.00	0.12 (−0.32, 0.56)	1.00	−0.15 (−0.33, 0.03)	0.54
Language	−0.27 (−0.70, 0.16)	1.00	0.04 (−0.03, 0.11)	1.00	0.50 (−0.15, 1.15)	0.78	−0.09 (−0.33, 0.15)	1.00
Visuospatial functions	−0.14 (−0.46, 0.18)	1.00	−0.05 (−0.11, 0.01)	0.60	0.23 (−0.25, 0.71)	1.00	0.05 (−0.17, 0.27)	1.00
CBI-R	−0.09 (−6.19, 6.01)	1.001	−0.73 (−1.79, 0.34)	1.00	4.32 (−4.53, 13.17)	1.00	1.49 (−1.74, 4.71)	1.00
	***MAPT* presymptomatic**				***MAPT* symptomatic**			
Global cognition	−0.27 (−1.67, 1.13)	1.00	0.10 (−0.19, 0.39)	1.00	0.49 (−1.90, 2.87)	1.00	0.44 (−0.15, 1.03)	0.84
Attention and processing speed	−0.005 (−0.38, 0.37)	1.00	−0.03 (−0.12, 0.05)	1.00	−0.18 (−0.80, 0.44)	1.00	−0.16 (−0.31, −0.0004)	0.29
Executive functions	−0.06 (−0.43, 0.31)	1.00	−0.01 (−0.10, 0.07)	1.00	0.11 (−0.49, 0.71)	1.00	0.13 (−0.02, 0.29)	0.60
Language	0.07 (−0.45, 0.59)	1.00	0.04 (−0.07, 0.15)	1.00	0.004 (−0.90, 0.91)	1.00	0.18 (−0.03, 0.38)	0.54
Visuospatial functions	−0.20 (−0.60, 0.21)	1.00	−0.08 (−0.16, 0.01)	0.49	0.20 (−0.46, 0.87)	1.00	−0.15 (−0.33, 0.03)	0.55
CBI-R	−0.63 (−8.23, 6.97)	1.00	0.95 (−0.75, 2.64)	1.00	−4.93 (−16.43, 6.56)	1.00	−0.98 (−3.76, 1.80)	1.00

β^{int}, *P*-value^{int} and corrected *P*-value^{int} at baseline: β, *P*-value, and corrected *P*-value for an interaction between *TMEM106B-rs1990622*^{G} allele dosage and gene-clinical status at time from baseline = 0. β^{int}, *P*-value^{int} and corrected *P*-value^{int} over time: β, *P*-value, and corrected *P*-value for a triple interaction between *TMEM106B-rs1990622*^{G} allele dosage, gene-clinical status, and time from baseline. Diagnoses *C9orf72* ($n = 45$): ALS = 7; bvFTD = 32; primary progressive aphasia = 3; parkinsonism = 1; other = 2. Diagnoses *GRN* ($n = 29$): bvFTD = 14; primary progressive aphasia = 12; parkinsonism = 1; other = 2. Diagnoses *MAPT* ($n = 13$): bvFTD = 13. Refer to Supplementary Table 6 for complete outputs of linear mixed-effects models including test statistics and degrees of freedom. Estimates in each domain are derived from a single linear mixed-effects model. CI = confidence interval; CBI-R = Cambridge Behaviour Inventory-Revised. Higher scores reflect greater behavioural impairment.

[a]Corrected for six tests (MMSE, attention and processing speed, executive functions, language, visuospatial functions, and CBI-R).

only in mutation carriers after accounting for education level.[77] This study did not include symptomatic mutation carriers. In addition to a longitudinal design, we included an extended GENFI sample and examined the interactions between *TMEM106B-rs1990622* and *GRN*, *C9orf72* and *MAPT* mutations accounting for the clinical status of individuals.

The lack of results in our non-carrier control group contrast with results from the population-based Rotterdam study, which showed lower volumes in left temporal regions associated with the *TMEM106B* risk allele in healthy older adults.[32] The difference in findings might be explained by the cross-sectional nature of that particular Rotterdam study cohort in contrast to our longitudinal design, differences in sample compositions, and most importantly a much larger sample size in the Rotterdam study. It was composed of healthy older adults ($n = 4413$) with a mean age of 65 years with 17.6% $rs1990622^{GG}$ participants, compared to the mean age of 47 years and 8.9% $rs1990622^{GG}$ participants in our control sample.

As the protective effects of *TMEM106B* on disease progression are most pronounced in *GRN* mutation carriers,[22] a larger number of individuals with *GRN* mutations homozygous for $rs1990622^{G}$ may remain asymptomatic throughout life or until a later age and simply do not show up in the clinic to participate in research studies.[22] This is strongly supported by the frequency of $rs1990622^{GG}$ individuals in *GRN* symptomatic carriers, which was 10% ($n = 3$), compared to 22.2% ($n = 10$) in symptomatic *C9orf72* carriers.

The study by Finch *et al.*[23] showed that in *GRN* mutation carriers, proportions of $rs1990622^{G}$ heterozygotes were significantly elevated relative to homozygotes, suggesting that the protective effect of *TMEM106B* follows a recessive pattern. However, results from our study are suggestive of an additive effect, and that the presence of one protective G allele confers some degree of protection. Our study examines FTD endophenotypes and includes both presymptomatic and symptomatic carriers in a longitudinal design, which might explain this difference. However, we could not perform any secondary stratified analyses in $rs1990622^{AG}$ and $rs1990622^{GG}$ groups due to few subjects in the symptomatic GG groups.

We acknowledge the limitations in this work. Although the sample size was sufficient for overall analyses, it was not sufficient to perform secondary stratified analyses in $rs1990622^{AG}$ and $rs1990622^{GG}$ carriers due to fewer $rs1990622^{GG}$ carriers. However, our main analyses, together with secondary survival and *post hoc* analysis with converters, strongly support additive effects of the G allele. The effects on memory function could not be tested in the full sample due to inconsistent tests between GENFI 1 and GENFI 2, however, we performed memory analysis in a subsample and also included MMSE as a measure of global cognition in addition to domain-specific scores for maximum coverage possible. Also, the visuospatial domain was tested using only one test, which might have reduced the sensitivity to detect changes in this domain.

In conclusion, *TMEM106B-rs1990622* strongly modifies the effect of autosomal dominant FTD mutations on the natural course of genetic FTD, particularly with TDP-43 pathology. Based on these findings, we recommend that *TMEM106B-rs1990622* should be assessed in clinical trials targeting *GRN* and *C9orf72*-related FTD due to its effect on common outcome measures of atrophy, biomarkers of neurodegeneration and cognition being used in these studies.

Data availability

The raw data of this project is part of GENFI. De-identified participant data can be accessed on reasonable request to the corresponding author and genfi@ucl.ac.uk.

Acknowledgements

We thank the research participants and their families for their contribution to the study. We also thank Jackie Poos for her guidance on the use of neuropsychological measures.

Funding

M.M. has received funding from two Canadian Institutes of Health Research project grants (MOP-327387 and PJT-175242) and from the Weston Brain Institute for the conduct of this study. S.S.M. has received salary support from the Centre for Brain Resilience and Recovery (CBRR). M.M. receives salary support from the Sunnybrook Foundation, as well as the Department of Medicine at Sunnybrook Health Sciences Centre and the University of Toronto. J.B.R. has received funding from the Wellcome Trust (103838; 220258) and is supported by the Cambridge University Centre for Frontotemporal Dementia, the Medical Research Council (MC_UU_00030/14; MR/T033371/1) and the National Institute for Health Research Cambridge Biomedical Research Centre (NIHR203312: BRC-1215-20014) and the Holt Fellowship. The views expressed are those of the authors and not necessarily those of the National Institute for Health Research or the Department of Health and Social Care. J.C.V.S., L.C.J. and H.S. are supported by a Dioraphte Foundation grant 09-02-03-00, Association for Frontotemporal Dementias Research Grant 2009, Netherlands Organization for Scientific Research grant HCMI 056-13-018, ZonMw Memorabel (Deltaplan Dementie, project number 733 051 042), ZonMw Onderzoeksprogramma Dementie (YOD-INCLUDED, project number 10510032120002), Alzheimer Nederland and the Bluefield Project. R.S-V. is supported by Alzheimer's Research UK Clinical Research Training Fellowship (ARUK-CRF2017B-2) and has received funding from Fundació Marató de TV3, Spain (grant no. 20143810). C.G. received funding from the EU Joint Programme-Neurodegenerative Disease Research-Prefrontals Vetenskapsrådet Dnr 529-2014-7504, Vetenskapsrådet 2019-0224, Vetenskapsrådet 2015-02926, Vetenskapsrådet 2018-02754, the Swedish Frontotemporal Dementia Inititative Schörling Foundation, Swedish Alzheimer Foundation, Swedish Brain Foundation, Swedish Dementia Foundation and Region Stockholm ALF-project. D.G. received support from the EU Joint Programme-Neurodegenerative Disease Research and the Italian Ministry of Health (PreFrontALS) grant 733051042. R.V. has received funding from the Mady Browaeys Fund for Research into Frontotemporal Dementia. J.L. received funding for this work by the Deutsche Forschungsgemeinschaft German Research Foundation under Germany's Excellence Strategy within the framework of the Munich Cluster for Systems Neurology (EXC 2145 SyNergy—ID 390857198). M.O. has received funding from Germany's Federal Ministry of Education and Research (BMBF). E.F. has received funding from a Canadian Institute of Health Research grant #327387. F.M. is supported by the Tau Consortium and has received funding from the Carlos III Health Institute (PI19/01637). M.B. is supported by a Fellowship award from the Alzheimer's Society, United Kingdom (AS-JF-19a-004-517). J.D.R. is supported by the Bluefield Project and the National Institute for Health and Care Research University College London Hospitals Biomedical Research Centre and has received funding from an MRC Clinician Scientist Fellowship (MR/M008525/1) and a Miriam Marks Brain Research UK Senior Fellowship. Several authors of this publication (J.C.V.S., M.S., R.V., A.d.M., M.O., R.V., J.D.R.) are members of the

European Reference Network for Rare Neurological Diseases (ERN-RND)—Project ID No 739510. This work was also supported by the EU Joint Programme-Neurodegenerative Disease Research GENFI-PROX grant [2019-02248; to J.D.R., M.O., B.B., C.G., J.C.V.S. and M.S.].

Competing interests

The authors report no competing interests.

Supplementary material

Supplementary material is available at *Brain* online.

Appendix 1

Further information on GENFI consortium members is provided in the Supplementary material.

GENFI consortium members

Rhian Convery, Sophie Goldsmith, Kiran Samra, David L. Thomas, Thomas Cope, Timothy Rittman, Maura Malpetti, Antonella Alberici, Enrico Premi, Roberto Gasparotti, Emanuele Buratti, Valentina Cantoni, Andrea Arighi, Chiara Fenoglio, Vittoria Borracci, Maria Serpente, Tiziana Carandini, Emanuela Rotondo, Giacomina Rossi, Giorgio Giaccone, Giuseppe Di Fede, Paola Caroppo, Sara Prioni, Veronica Redaelli, Johanna Krüger, Miguel Castelo-Branco, Ron Keren, Christen Shoesmith, Robart Bartha, Rosa Rademakers, Jackie Poos, Janne M. Papma, Lucia Giannini, Liset de Boer, Julie de Houwer, Rick van Minkelen, Yolande Pijnenburg, Benedetta Nacmias, Camilla Ferrari, Cristina Polito, Gemma Lombardi, Valentina Bessi, Enrico Fainardi, Stefano Chiti, Mattias Nilsson, Henrik Viklund, Melissa Taheri Rydell, Vesna Jelic, Linn Öijerstedt, Tobias Langheinrich, Albert Lladó, Anna Antonell, Jaume Olives, Mircea Balasa, Nuria Bargalló, Sergi Borrego-Ecija, Ana Verdelho, Carolina Maruta, Tiago Costa-Coelho, Gabriel Miltenberger, Frederico Simões do Couto, Alazne Gabilondo, Ioana Croitoru, Mikel Tainta, Myriam Barandiaran, Patricia Alves, Benjamin Bender, David Mengel, Lisa Graf, Annick Vogels, Mathieu Vandenbulcke, Philip Van Damme, Rose Bruffaerts, Koen Poesen, Pedro Rosa-Neto, Maxime Montembault, Agnès Camuzat, Alexis Brice, Anne Bertrand, Aurélie Funkiewiez, Daisy Rinaldi, Dario Saracino, Olivier Colliot, Sabrina Sayah, Catharina Prix, Elisabeth Wlasich, Olivia Wagemann, Sonja Schönecker, Alexander Maximilian Bernhardt, Anna Stockbauer, Jolina Lombardi, Sarah Anderl-Straub, Adeline Rollin, Gregory Kuchcinski, Maxime Bertoux, Thibaud Lebouvier, Vincent Deramecourt, João Durães, Marisa Lima, Maria João Leitão, Maria Rosario Almeida, Miguel Tábuas-Pereira, Sónia Afonso, João Lemos.

References

1. Seelaar H, Rohrer JD, Pijnenburg YAL, Fox NC, Van Swieten JC. Clinical, genetic and pathological heterogeneity of frontotemporal dementia: A review. *J Neurol Neurosurg Psychiatry*. 2011; 82:476-486.
2. DeJesus-Hernandez M, Mackenzie IR, Boeve BF, et al. Expanded GGGGCC hexanucleotide repeat in noncoding region of C9ORF72 causes chromosome 9p-linked FTD and ALS. *Neuron*. 2011;72:245-256.
3. Renton AE, Majounie E, Waite A, et al. A hexanucleotide repeat expansion in C9ORF72 is the cause of chromosome 9p21-linked ALS-FTD. *Neuron*. 2011;72:257.
4. Baker M, Mackenzie IR, Pickering-Brown SM, et al. Mutations in progranulin cause tau-negative frontotemporal dementia linked to chromosome 17. *Nature*. 2006;442:916-919.
5. Cruts M, Gijselinck I, Van Der Zee J, et al. Null mutations in progranulin cause ubiquitin-positive frontotemporal dementia linked to chromosome 17q21. *Nature*. 2006;442:920-924.
6. Hutton M, Lendon CL, Rizzu P, et al. Association of missense and 5′-splice-site mutations in tau with the inherited dementia FTDP-17. *Nature*. 1998;393:702-705.
7. Pottier C, Ravenscroft TA, Sanchez-Contreras M, Rademakers R. Genetics of FTLD: Overview and what else we can expect from genetic studies. *J Neurochem*. 2016;138:32-53.
8. Albani D, Agosta F, Batelli S, Borroni B, Benussi A, Padovani A. Phenotypic heterogeneity of monogenic frontotemporal dementia. *Front Aging Neurosci*. 2015;7:171.
9. Kelley BJ, Haidar W, Boeve BF, et al. Prominent phenotypic variability associated with mutations in progranulin. *Neurobiol Aging*. 2009;30:739.
10. Snowden JS, Rollinson S, Thompson JC, et al. Distinct clinical and pathological characteristics of frontotemporal dementia associated with C9ORF72 mutations. *Brain*. 2012;135(Pt 3):693-708.
11. Pasternak M, Mirza SS, Mutsaerts H, et al. A longitudinal analysis of cerebral blood flow changes in genetic frontotemporal dementia: Results from GENFI. *Alzheimer's Dement*. 2023;19(S3): e067181.
12. Fumagalli GG, Basilico P, Arighi A, et al. Distinct patterns of brain atrophy in Genetic Frontotemporal Dementia Initiative (GENFI) cohort revealed by visual rating scales. *Alzheimers Res Ther*. 2018;10:46.
13. Cash DM, Bocchetta M, Thomas DL, et al. Patterns of gray matter atrophy in genetic frontotemporal dementia: Results from the GENFI study. *Neurobiol Aging*. 2018;62:191-196.
14. Poos JM, Macdougall A, Van Den Berg E, et al. Longitudinal cognitive changes in genetic frontotemporal dementia within the GENFI cohort. *Neurology*. 2022;99:E281-E295.
15. Rohrer JD, Woollacott IOC, Dick KM, et al. Serum neurofilament light chain protein is a measure of disease intensity in frontotemporal dementia. *Neurology*. 2016;87:1329-1336.
16. Rojas JC, Wang P, Staffaroni AM, et al. Plasma neurofilament light for prediction of disease progression in familial frontotemporal lobar degeneration. *Neurology*. 2021;96:e2296-e2312.
17. Staffaroni AM, Quintana M, Wendelberger B, et al. Temporal order of clinical and biomarker changes in familial frontotemporal dementia. *Nat Med*. 2022;28:2194.
18. Warren JD, Rohrer JD, Rossor MN. Clinical review. Frontotemporal dementia. *BMJ*. 2013;347:f4827.
19. Desmarais P, Rohrer JD, Nguyen QD, et al. Therapeutic trial design for frontotemporal dementia and related disorders neurodegeneration. *J Neurol Neurosurg Psychiatry*. 2019;90:412-423.
20. Trajanoska K, Bhérer C, Taliun D, Zhou S, Richards JB, Mooser V. From target discovery to clinical drug development with human genetics. *Nature*. 2023;620:737-745.
21. Van Deerlin VM, Sleiman PMA, Martinez-Lage M, et al. Common variants at 7p21 are associated with frontotemporal lobar degeneration with TDP-43 inclusions. *Nat Genet*. 2010;42:234.
22. Nicholson AM, Rademakers R. What we know about TMEM106B in neurodegeneration. *Acta Neuropathol*. 2016;132:639-651.
23. Finch N, Carrasquillo MM, Baker M, et al. TMEM106B regulates progranulin levels and the penetrance of FTLD in GRN mutation carriers. *Neurology*. 2011;76:467-474.

24. van Blitterswijk M, Mullen B, Wojtas A, et al. Genetic modifiers in carriers of repeat expansions in the C9ORF72 gene. *Mol Neurodegener*. 2014;9:38.
25. Pottier C, Zhou X, Perkerson RB, et al. Potential genetic modifiers of disease risk and age at onset in patients with frontotemporal lobar degeneration and GRN mutations: A genome-wide association study. *Lancet Neurol*. 2018;17:548-558.
26. Nicholson AM, Finch NA, Wojtas A, et al. TMEM106B p.T185S regulates TMEM106B protein levels: Implications for frontotemporal dementia. *J Neurochem*. 2013;126:781.
27. Lattante S, Le Ber I, Galimberti D, et al. Defining the association of TMEM106B variants among frontotemporal lobar degeneration patients with GRN mutations and C9orf72 repeat expansions. *Neurobiol Aging*. 2014;35:2658.e1-2658.e5.
28. van Blitterswijk M, Mullen B, Nicholson AM, et al. TMEM106B protects C9ORF72 expansion carriers against frontotemporal dementia. *Acta Neuropathol*. 2014;127:397-406.
29. Van Der Zee J, Van Broeckhoven C. TMEM106B a novel risk factor for frontotemporal lobar degeneration. *J Mol Neurosci*. 2011; 45:516--5121.
30. Rollinson S, Mead S, Snowden J, et al. Frontotemporal lobar degeneration genome wide association study replication confirms a risk locus shared with amyotrophic lateral sclerosis. *Neurobiol Aging*. 2011;32:758.e1-758.e7.
31. Harding SR, Bocchetta M, Gordon E, et al. Letter: The TMEM106B risk allele is associated with lower cortical volumes in a clinically diagnosed frontotemporal dementia cohort. *J Neurol Neurosurg Psychiatry*. 2017;88:997.
32. Adams HHH, Verhaaren BFJ, Vrooman HA, et al. TMEM106B influences volume of left-sided temporal lobe and interhemispheric structures in the general population. *Biol Psychiatry*. 2014;76:503-508.
33. Tropea TF, Mak J, Guo MH, et al. TMEM106B effect on cognition in Parkinson's disease and frontotemporal dementia. *Ann Neurol*. 2019;85:801-881.
34. Cruchaga C, Graff C, Chiang HH, et al. TMEM106B gene polymorphism is associated with age at onset in granulin mutation carriers and plasma granulin protein levels. *Arch Neurol*. 2011;68:581.
35. Chang A, Xiang X, Wang J, et al. Homotypic fibrillization of TMEM106B across diverse neurodegenerative diseases. *Cell*. 2022;185:1346-1355.e15.
36. Rohrer JD, Nicholas JM, Cash DM, et al. Presymptomatic cognitive and neuroanatomical changes in genetic frontotemporal dementia in the genetic frontotemporal dementia initiative (GENFI) study: A cross-sectional analysis. *Lancet Neurol*. 2015; 14:253-262.
37. Blauwendraat C, Faghri F, Pihlstrom L, et al. NeuroChip, an updated version of the NeuroX genotyping platform to rapidly screen for variants associated with neurological diseases HHS public access. *Neurobiol Aging*. 2017;57:247.e9–247.e13.
38. Purcell S, Neale B, Todd-Brown K, et al. PLINK: A tool set for whole-genome association and population-based linkage analyses. *Am J Hum Genet*. 2007;81:559-575.
39. Manichaikul A, Mychaleckyj JC, Rich SS, et al. Robust relationship inference in genome-wide association studies. *Bioinformatics*. 2010;26:2867-2873.
40. Jin Y, Schaffer AA, Feolo M, Holmes JB, Kattman BL. GRAF-pop: A fast distance-based method to infer subject ancestry from multiple genotype datasets without principal components analysis. 2019;9:2447-2461.
41. Conomos MP, Miller MB, Thornton TA. Robust inference of population structure for ancestry prediction and correction of stratification in the presence of relatedness. *Genet Epidemiol*. 2015;39:276-293.
42. Gogarten SM, Sofer T, Chen H, et al. Genetic association testing using the GENESIS R/bioconductor package. *Bioinformatics*. 2019; 35:5346-5348.
43. Cattell RB. The scree test for the number of factors. *Multivariate Behav Res*. 1966;1:245-276.
44. Taliun D, Harris DN, Kessler MD, et al. (2019) Sequencing of 53,831 diverse genomes from the NHLBI TOPMed Program. *bioRxiv*. [Preprint] doi:https://doi.org/10.1101/563866
45. Gaser C, Dahnke R, Thompson PM, et al. (2023).CAT—A Computational Anatomy Toolbox for the analysis of structural MRI data. *bioRxiv*. [Preprint] doi:https://doi.org/10.1101/2022.06.11.495736
46. Ashburner J, Friston KJ. Diffeomorphic registration using geodesic shooting and Gauss-Newton optimisation. *Neuroimage*. 2011;55:954-967.
47. Malone IB, Leung KK, Clegg S, et al. Accurate automatic estimation of total intracranial volume: A nuisance variable with less nuisance. *Neuroimage*. 2015;104:366-372.
48. van der Ende EL, Meeter LH, Poos JM, et al. Serum neurofilament light chain in genetic frontotemporal dementia: A longitudinal, multicentre cohort study. *Lancet Neurol*. 2019;18:1103-1111.
49. Morris JC, Weintraub S, Chui HC, et al. The Uniform Data Set (UDS): Clinical and cognitive variables and descriptive data from Alzheimer Disease Centers. *Alzheimer Dis Assoc Disord*. 2006;20:210-216.
50. Corrigan JD, Hinkeldey NS. Relationships between parts A and B of the trail making test. *J Clin Psychol*. 1987;43:402-409.
51. Tombaugh TN, Kozak J, Rees L. Normative data stratified by age and education for two measures of verbal fluency: FAS and animal naming. *Arch Clin Neuropsychol*. 1999;14:167-177.
52. Wechsler D. *Wechsler adult intelligence scale-revised*. Psychological Corporation; 1981.
53. Folstein MF, Folstein SE, McHugh PR. Mini-mental state": A practical method for grading the cognitive state of patients for the clinician. *J Psychiatr Res*. 1975;12:189-198.
54. Wechsler D. Wechsler D. WMS-IV—Wechsler Memory Scale | Fourth Edition | Pearson Assessments US. 2009. Accessed 20 October 2024. https://www.pearsonassessments.com/store/usassessments/en/Store/Professional-Assessments/Cognition-%26-Neuro/Wechsler-Memory-Scale-%7C-Fourth-Edition/p/100000281.html
55. Grober E, Sanders AE, Hall C, Lipton RB. Free and cued selective reminding identifies very mild dementia in primary care. *Alzheimer Dis Assoc Disord*. 2010;24:284.
56. Gavett BE, Gurnani AS, Saurman JL, et al. Practice effects on story memory and list learning tests in the neuropsychological assessment of older adults. *PLoS One*. 2016;11:e0164492.
57. Wear HJ, Wedderburn CJ, Mioshi E, et al. The Cambridge behavioural inventory revised. *Dement Neuropsychol*. 2008;2:102-107.
58. Cox RW. AFNI: Software for analysis and visualization of functional magnetic resonance neuroimages. *Comput Biomed Res*. 1996;29:162-173.
59. Chen G, Saad ZS, Britton JC, Pine DS, Cox RW. Linear mixed-effects modeling approach to FMRI group analysis. *Neuroimage*. 2013;73:176-190.
60. Cox RW, Chen G, Glen DR, Reynolds RC, Taylor PA. FMRI clustering in AFNI: False-positive rates redux. *Brain Connect*. 2017;7: 152-171.
61. Rorden C, Brett M. Stereotaxic display of brain lesions. Accessed 26 March 2024. www.fil.ion.ucl.ac.uk/spm/
62. Notter MP, Gale D, Herholz P, Markello R, Notter-Bielser M-L, Whitaker K. AtlasReader: A Python package to generate coordinate tables, region labels, and informative figures from statistical MRI images. *J Open Source Softw*. 2019;4:1257.

63. Popuri K, Dowds E, Faisal Beg M, et al. Gray matter changes in asymptomatic C9orf72 and GRN mutation carriers. *NeuroImage Clin*. 2018;18:591-598.
64. Benussi A, Premi E, Gazzina S, et al. Progression of behavioral disturbances and neuropsychiatric symptoms in patients with genetic frontotemporal dementia. *JAMA Netw Open*. 2021;4: e2030194.
65. Masellis M, Momeni P, Meschino W, et al. Novel splicing mutation in the progranulin gene causing familial corticobasal syndrome. *Brain*. 2006;129:3115-3123.
66. Seeley WW. Anterior insula degeneration in frontotemporal dementia. *Brain Struct Funct*. 2010;214:465-475.
67. Seeley WW, Crawford RK, Zhou J, Miller BL, Greicius MD. Neurodegenerative diseases target large-scale human brain networks. *Neuron*. 2009;62:42-52.
68. Saracino D, Dorgham K, Camuzat A, et al. Original research: Plasma NfL levels and longitudinal change rates in C9orf72 and GRN-associated diseases: From tailored references to clinical applications. *J Neurol Neurosurg Psychiatry*. 2021;92: 1278.
69. Lima M, Tábuas-Pereira M, Duro D, et al. Neuropsychological features of progranulin-associated frontotemporal dementia: A nested case-control study. *Neural Regen Res*. 2021;16:910.
70. Hsiung GYR, Dejesus-Hernandez M, Feldman HH, et al. Clinical and pathological features of familial frontotemporal dementia caused by C9ORF72 mutation on chromosome 9p. *Brain*. 2012; 135:709-722.
71. Chen-Plotkin AS, Unger TL, Gallagher MD, et al. TMEM106B, the risk gene for frontotemporal dementia, is regulated by the microRNA-132/212 cluster and affects progranulin pathways. *J Neurosci*. 2012;32:11213-11227.
72. Feng T, Lacrampe A, Hu F. Physiological and pathological functions of TMEM106B: A gene associated with brain aging and multiple brain disorders. *Acta Neuropathol*. 2021;141:327.
73. Werner G, Damme M, Schludi M, et al. Loss of TMEM 106B potentiates lysosomal and FTLD-like pathology in progranulin-deficient mice. *EMBO Rep*. 2020;21:e50241.
74. Zhou X, Brooks M, Jiang P, et al. Loss of Tmem106b exacerbates FTLD pathologies and causes motor deficits in progranulin-deficient mice. *EMBO Rep*. 2020;21:e50197.
75. Feng T, Mai S, Roscoe JM, et al. Loss of TMEM 106B and PGRN leads to severe lysosomal abnormalities and neurodegeneration in mice. *EMBO Rep*. 2020;21:e50219.
76. Mao F, Robinson JL, Unger T, et al. TMEM106B modifies TDP-43 pathology in human ALS brain and cell-based models of TDP-43 proteinopathy. *Acta Neuropathol*. 2021;142:629-642.
77. Premi E, Grassi M, van Swieten J, et al. Cognitive reserve and TMEM106B genotype modulate brain damage in presymptomatic frontotemporal dementia: A GENFI study. *Brain*. 2017; 140:1784-1791.